Article

Celecoxib-Nicotinamide Co-Crystal Revisited: Can Entropy Control Co-Crystal Formation?

Si-Wei Zhang, Andrew P. J. Brunskill, Eric Schwartz, and Shuwen Sun

Cryst. Growth Des., **Just Accepted Manuscript** • DOI: 10.1021/acs.cgd.7b00308 • Publication Date (Web): 10 Apr 2017

Celecoxib-Nicotinamide Co-Crystal Revisited: Can Entropy Control Co-Crystal Formation?

Si-Wei Zhang, Andrew P. J. Brunskill, Eric Schwartz, Shuwen Sun

Department of Process Research & Development, Merck & Co., Inc.,

126 East Lincoln Avenue, Rahway, NJ 07065 USA

ABSTRACT: The co-crystal of celecoxib-nicotinamide has been revisited to reveal its crystal structure and unusual formation properties. Gibbs free energy and enthalpy of formation at 25 °C were determined by solubility and thermal analysis. The formation of celecoxib-nicotinamide was found to be an endothermic process and driven by entropy, a mechanism different from many reported co-crystals but in agreement with previously reported lattice energy calculation. The co-crystal is stable only *above* a transition temperature as predicted from thermodynamic data and confirmed experimentally. This formation mechanism brings new opportunities into co-crystal research from structural prediction to process development, and enriches our understanding on the nature of co-crystallization.

KEYWORDS: Co-crystal, celecoxib, nicotinamide, thermodynamics, formation energy

INTRODUCTION

Co-crystallization has evolved as a general strategy to expand the number of solid forms available for pharmaceuticals[1-4] or other materials[5] and to improve their physicochemical properties.[5-8] The formation of co-crystals does not require the presence of ionizable groups in co-crystal formers, making co-crystallization a more versatile method in crystal engineering than salt formation. [9] Accompanying the discovery and structural solution of an increasing number of co-crystals, more efforts have been focused on their thermodynamic formation properties.[10-14] In-depth understanding of these important characteristics will benefit co-crystal research in both the discovery and development phases. Acquiring formation enthalpies (ΔH_f) of co-crystals by experimental[13] or computational[15] methods will aid in the structural prediction and rational design of co-crystals.[15-17] Furthermore, exploration of the phase diagrams of co-crystals, including binary[18-20] and ternary[21-23] phase diagrams, provides guidance on their process development.

The key to understanding the thermodynamics of co-crystals is the formation Gibbs free energy (ΔG_f) which determines the stability of a co-crystal. Although ΔG_f can be experimentally measured for existing co-crystals,[10-12] forecasting ΔG_f is of great interest for crystal structure prediction. However, computational calculation of ΔG_f is costly.[24] As a result, the computationally inexpensive lattice energy and formation energy (ΔE_f) were often used instead of ΔG_f in structural prediction.[15,25] It is noted that the difference between ΔE_f and ΔG_f is the entropy term, as ΔE_f is approximate to ΔH_f at ambient conditions.[26] Therefore, correlating ΔE_f with co-crystal stability assumes that enthalpy is the major component of free energy and the main driving force of co-crystallization.

The validity of the assumption that co-crystallization is enthalpy controlled has been examined both experimentally and computationally. Indeed, although only limited experimental data is available, co-crystallization is shown to be a competition between an enthalpy term favorable for co-crystal formation and an entropy term against the formation.[11,12] However, a few exceptions can be found, especially from computational calculations.[27] In a recent study, Chan *et al*. demonstrated the ability to calculate, *ab initio*, the ΔE_f of a series of nicotinamide (NIC) co-crystals based on dispersion-corrected density functional theory (DFT-D). In this study, it was found that 30 out of 31 NIC co-crystals have negative ΔE_f in favor of co-crystallization.[15] The co-crystal formed between NIC and celecoxib (CEL),[28] a COX-2 selective nonsteroidal anti-inflammatory drug (NSAID), was left as an outlier. Such exceptions were often attributed to the inadequacy of computational methods or simply ignored.

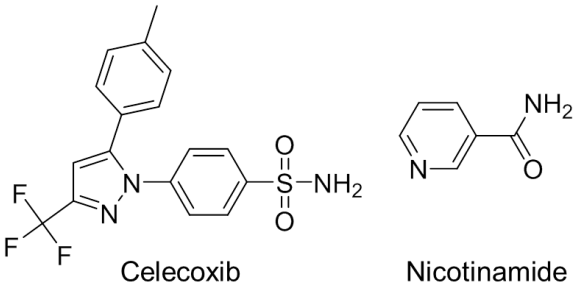

Scheme 1. Structures of celecoxib (CEL) and nicotinamide (NIC)

In this work, the CEL-NIC co-crystal was revisited and its crystal structure was determined by X-ray crystallography. The structure corrects several errors in the structure previously determined using X-ray powder data.[28] The newly determined structure agrees with the *in silico* optimized structure reported by Chan *et al*.[15] which allows the comparison between experimental and computational studies. ΔG_f and ΔH_f of the co-crystal were determined from the solubility and thermal properties of the co-crystal and a physical mixture of component crystals. At 25 °C, CEL-NIC was found to be energetically stable (ΔG_f = -0.7 (0.1) J/g) with an endothermic formation (ΔH_f = +13 (3) J/g) that agrees with lattice energy calculation, indicating that the co-crystallization is driven by entropy (ΔS_f = +0.05 J/g). The existence of a transition

temperature (T_t) below 25 °C between CEL-NIC and its components was predicted from thermodynamic data and was confirmed by the inverted stability between the co-crystal and components observed between 4 °C and 25 °C. CEL-NIC is stable only *above* this temperature, unlike other enthalpy-controlled co-crystals which are usually stable *below* a transition temperature. The formation of CEL-NIC is different from other co-crystals with reported formation properties, which challenges the usage of ΔE_f or ΔH_f as the only indication of co-crystal formation. This discovery enriches the understanding on the nature of co-crystal formation, and is relevant to structural prediction and process development of co-crystals.

MATERIAL AND METHODS

Compounds and solvents. Celecoxib (the most stable polymorph[29]) was purchased from AstaTech (Bristol, PA, USA). Nicotinamide (the most stable polymorph[30]) was purchased from Acros (Geel, Belgium). Both materials were used as received. All solvents were of HPLC grade and purchased from Sigma-Aldrich (St. Louis, MO, USA). Analytical standards of nicotinamide and celecoxib were purchased from Sigma-Aldrich and European Pharmacopoeia Reference Standards (EDQM, Strasbourg, France), respectively.

X-ray diffraction experiments. Powder X-ray diffraction (PXRD) measurements were carried out on a Panalytical (Natick, MA, USA) X-pert Pro PW3040 diffractometer with an X'celerator detector (Cu Kα radiation, voltage 45 kV, and current 40 mA). Approximately 5 mg of powder was sprinkled on the surface of a zero background silicon (510) sample holder and scanned from 2 to 40° 2θ at a speed of 8.4°/min and a step size of 0.02°. Single-crystal X-ray diffraction (SCXRD) evaluation and data collection were performed at -173 °C and 25 °C on a Bruker

(Madison, WI, USA) SMART Apex II diffractometer with Cu Kα radiation, and the crystal structure was solved using a standard procedure (see the Supporting Information for details).

Thermal analysis. Differential scanning calorimetry (DSC) was conducted with a TA Instruments (New Castle, DE, USA) Discovery unit under 50 mL/min N_2 purge. In a typical run, 5 – 10 mg sample in a Tzero Aluminum pan was heated at 10 °C/min to 185 °C to measure the temperature and heat of melting, cooled at 10 °C/min, and heated again at 10 °C/min to record the glass transition temperature of the melt. Results are reported as the average of at least three replicated experiments.

High-performance liquid chromatography (HPLC) method. HPLC was performed on an Agilent (Santa Clara, CA, USA) 1100 HPLC system equipped with a diode array detector. The separation was carried out on a 4.6 mm × 150 mm, 2.7 μm Ascentis Express fused-core C18 column (Sigma-Aldrich). The mobile phase consisted of (A) 0.1% phosphoric acid and (B) acetonitrile. The gradient started with 5% B and ramped up to 95% B in 3 min, followed by a 3 min hold and a 3 min re-equilibration. For both CEL and NIC, UV detection was carried out at wavelength of 220 nm. The external standards were 0.2 mg/ml solutions in acetonitrile. The injection volume was set as 5 μL. The concentrations were calculated with an established calibration curve ranging from 0.1 μg/ml to 0.24 mg/ml. The HPLC method was validated by linearity and recovery.

Preparation of co-crystal and physical mixture. Co-crystals were obtained by dissolving 0.15 M CEL and NIC in chloroform/heptane 5/1 (v/v) at 65 °C. Hot solution was cooled to 50 °C, seeded with co-crystal, and cooled to room temperature at a rate of 1 °C/min. Single crystals were acquired by spontaneously cooling a hot chloroform solution of 0.5 M CEL and NIC to room temperature. To prepare a physical mixture of CEL and NIC crystals for DSC analysis,

each material was lightly ground in a mortar prior to mixing. The ground powders were mixed at 1:1 molar ratio with a Barnstead Thermolyne (Dubuque, IA, USA) Maxi Mix II vortex mixer at the maximum speed for 1 minute. The final mixture was analyzed by PXRD to ensure that it contained only the component crystals and no co-crystals, and was used immediately for subsequent DSC analysis.

Slurry experiments. To prepare a suspension for solubility measurement or phase conversion, excess amount of each solid was added into the selected solvent. The suspension was then held in a circulated metal block and magnetically stirred at 500 rpm. Temperature was controlled through circulating water by a Julabo circulator (Allentown, PA, USA) with accuracy of ±0.1 °C. Aliquots of the suspension were withdrawn at predetermined intervals and filtered through a 0.22 μm PTFE syringe filter. Phase of solid residue was immediately determined after filtration by PXRD. Concentration of CEL or NIC in the filtrate was determined by HPLC. Results are reported as the average of at least three replicated experiments.

Formation properties of co-crystal. The formation property of a co-crystal AB (1:1 stoichiometry) is defined in reference to equation 1:

$$A + B \rightarrow AB \quad (1)$$

where A and B are the crystal of component A (CEL) and the crystal of component B (NIC), respectively. The formation volume (ΔV_f) of a co-crystal (1:1 stoichiometry) is calculated using equation 2:[31]

$$\Delta V_f = V_{AB} - [0.5\ V_A + 0.5\ V_B] \quad (2)$$

where V_{AB}, V_A, and V_B are the volumes of one molecule (including void space) in the cocrystal, the component crystal A, and the component crystal B, respectively. V is calculated from crystallographic data using $V = V_{cell}/n$, where V_{cell} is the volume of the unit cell and n the number

of molecules there in. In this work, one "molecule" of co-crystal AB consists of 0.5 molecules of A and 0.5 of B. To avoid the ambiguity on the definition of one molecule, ΔV_f is also reported in the unit of cm^3/kg per co-crystal.[31]

Equation 3 is used to determine the formation enthalpy (ΔH_f):[13]

$$\Delta H_f = \Delta H_{m(A+B)} (T_S \rightarrow T_L) - \Delta H_{m(AB)} (T_S \rightarrow T_L) \quad (3)$$

where T_S (25 °C) is a temperature at which the co-crystal and the physical mixture of component crystals are solid and at which ΔH_f is evaluated, T_L (180 °C) is a temperature at which the co-crystal and the physical mixture are both melted to the same liquid, $\Delta H_{m(A+B)} (T_S \rightarrow T_L)$ and $\Delta H_{m(AB)} (T_S \rightarrow T_L)$ are the corresponding enthalpies of melting.

The formation energy (ΔE_f) is related to ΔH_f through equation 4 (P is pressure):

$$\Delta E_f = \Delta H_f + P\Delta V_f \quad (4)$$

Equation 5 is used to determine the formation Gibbs free energy (ΔG_f) at experimental temperature (25 °C):[11]

$$\Delta G_f = -RTln(C_{A(A+B)} / C_{A(AB+B)}) \quad (5)$$

where R is the gas constant, C_A is the concentration of CEL in a solution in equilibrium with the solids of physical mixture (A+B), or in equilibrium with the co-crystal and excess NIC (AB+B). Physical mixture (A+B) was used since the solubility of CEL was found to be related to the concentration of NIC, which will be discussed in the Results and Discussion section. Co-crystal and NIC (AB+B) were the solid residue from the incongruent dissolution of co-crystal in the testing solvent, chloroform. Molar concentration was used instead of activity for simplicity.

Finally, the entropy of formation (ΔS_f) can be determined from equation 6:

$$\Delta G_f = \Delta H_f - T\Delta S_f \quad (6)$$

Determinations of the change of hydrogen-bond length upon co-crystallization (ΔR_{HB}) can be found in supplementary information.

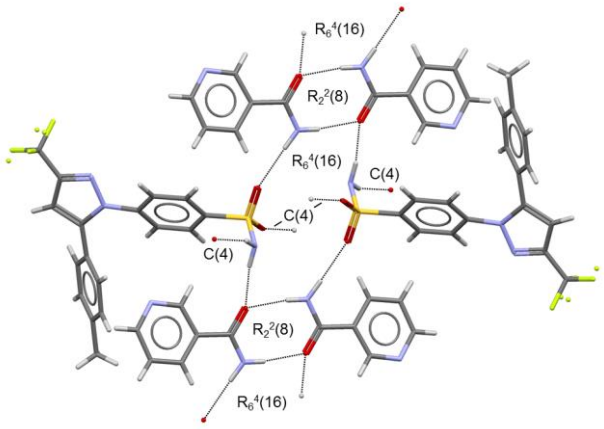

Figure 1. Hydrogen bonds in CEL-NIC co-crystal demonstrated by the 22 °C structure.

RESULTS AND DISCUSSION

Crystal structure. Single crystal structure of CEL-NIC was solved at both -173 °C and 22 °C. Relevant crystallographic data are shown in Table 1. In the 22 °C structure (Figure 1), NIC molecules form amide-amide $R_2^2(8)$ dimers.[32,33] NIC dimers are linked by CEL molecules (amide H – sulfonyl O; sulfonamide H – amide O) along the *b* direction to form infinite ribbons. In addition, these ribbons are stacked along the *a* direction and stabilized by the C(4) chain formed between CEL molecules (sulfonamide H – sulfonyl O). The -173 °C structure has the same hydrogen bond patterns as the 22 °C structure. The crystal volume shrinks by approximately 3% from 22 °C to -173 °C (thermal expansion coefficient $\alpha_V = 1.6 \times 10^{-4}$ °C $^{-1}$), which is comparable with NIC and other NIC co-crystal formers.[31] Disordered trifluoromethyl groups are observed at 22 °C but not at -173 °C. It should be noted that the molecular conformation in our single crystal structure is different from the reported powder structure, differing in the orientation of the sulfonamide group of CEL and the amide group of NIC.[28] The crystal structure is

Table 1. Crystallographic information for CEL-NIC co-crystal

T, °C	-173 (2)	22 (2)
Wavelength, Å	1.54178	1.54178
Cryst system	monoclinic	monoclinic
Space group	*P* 2_1/n	*P* 2_1/n
Cryst size, mm^3	0.2×0.04×0.01	0.2×0.04×0.01
a, Å	5.1077(3)	5.1908(2)
b, Å	9.8609(5)	9.9244(4)
c, Å	46.021(2)	46.3893(16)
α, deg	90	90
β, deg	91.1948(19)	92.2545(15)
γ, deg	90	90
V, Å^3	2317.41	2387.92
Z	4	4
ρ, cm^3/kg	1.443	1.401

consistent with the structure proposed by Chan *et al*. from a thorough conformational search and lattice energy minimization starting from the powder structure.[15]

A remarkable property of NIC co-crystals is their looser molecular packing and shorter hydrogen bonds relative to the component crystals.[31] CEL-NIC follows the same trend. We demonstrate this from its formation volume (ΔV_f) and the change of hydrogen-bond length upon co-crystallization (ΔR_{HB}). For determination of ΔV_f, molecular volumes of CEL-NIC and its components were acquired from room temperature crystal structures (CEL: CSD# DIBBUL;[34] NIC: CSD# NICOAM02;[35] both are the most stable polymorph). ΔV_f of CEL-NIC is 18.2 Å^3/molecule or 43.6 cm^3/kg, which indicates that the co-crystal occupies a volume 6.5% larger than individual components. Compared to other NIC co-crystals, CEL-NIC has one of the largest expansions in volume.[31] Despite the increase in volume, the average hydrogen bond length in CEL-NIC is shorter than the components (ΔR_{HB} = -0.1 Å; see the Supporting Information for details), in agreement with other NIC co-crystals.

Table 2. Thermal properties of CEL, NIC, 1:1 physical mixture and co-crystal

Phase	T_m, °C	ΔH_m, J/g	T_g, °C
Celecoxib	162.3 (0.3)	101.9 (0.7)	54.4 (0.1)
Nicotinamide	128.4 (0.1)	196.3 (0.4)	–[a]
1:1 physical mixture	107.8 (0.1)	111.6 (0.5)	21.9 (0.9)
Co-crystal	128.3 (0.1)	101.1 (0.3)	21.1 (0.1)

[a] T_g could not be measured due to crystallization

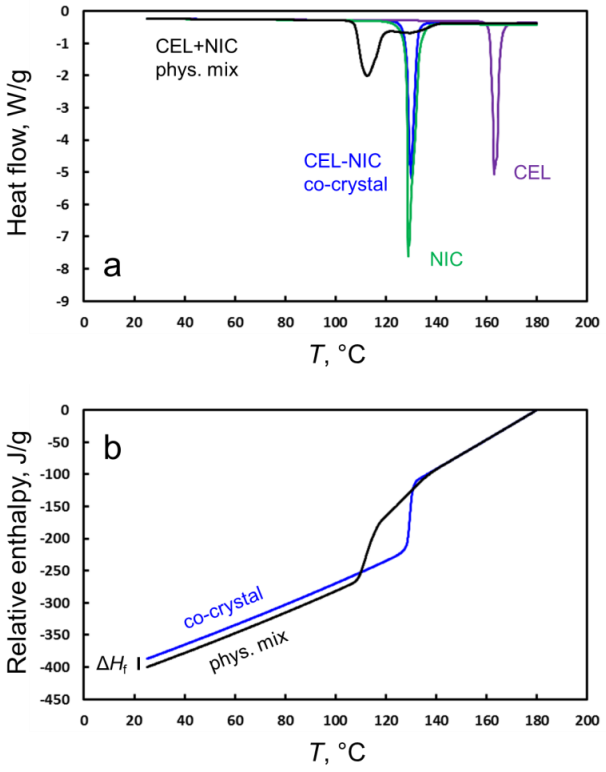

Figure 2. (a) DSC melting endotherms of CEL-NIC co-crystal, CEL, NIC, and a physical mixture of CEL and NIC at 1:1 molar ratio. (b) Relative enthalpies between co-crystal and the physical mixture. ΔH_f is the formation enthalpy of co-crystal (+13(3) J/g at 25 °C).

Determination of ΔH_f from thermal analysis. DSC traces of the co-crystal, component crystals, and a physical mixture of component crystals in 1:1 ratio are shown in Figure 2a, while related thermal properties are recorded in Table 2. Our results are in good agreement with existing data on CEL,[36] NIC,[13] and the co-crystal.[28] Thermogravimetric analysis shows no significant weight loss for CEL or NIC up to 180 °C, indicating that the melting data are unaffected by thermal decomposition. The T_g values in Table 2 are the glass transition temperatures observed during the second heating of the liquids produced by melting the crystals. The similar T_g values between co-crystal and physical mixture are consistent with similar chemical compositions of the crystalline samples before melting.

Figure 2b demonstrates the determination of the formation enthalpy (ΔH_f) of CEL-NIC co-crystal.[13] To obtain the formation enthalpy, heat flow data of the co-crystal and the physical mixture in Figure 2a were integrated from a common liquid-state temperature (180 °C) down to a common solid-state temperature (25 °C). Given that both the co-crystal and the physical mixture melted to the same liquid at 180 °C, the enthalpy difference of the co-crystal relative to the physical mixture is its formation enthalpy (equation 3). For CEL-NIC, ΔH_f was determined to be +13 (3) J/g at 25 °C, which indicates that the co-crystal has higher enthalpy compared with the physical mixture. Although ΔH_f was determined at a specific temperature, it is expected to be insensitive to temperature change around that temperature. This is supported by the similarity in the slope of relative enthalpies around 25 °C (Figure 2b). Note that both CEL and NIC used in this study are the most stable polymorph at ambient conditions; ΔH_f will change accordingly if a different polymorph is used as the starting material.[11]

It is of interest to compare the ΔH_f acquired from experimental and computational methods. ΔH_f is comparable to formation energy (ΔE_f) for a typical NIC co-crystal under ambient

conditions.[26] As in the case of CEL-NIC, the difference ($P\Delta V_f$) is about 4 mJ/g at 1 bar (equation 4), which is negligible compared with the magnitude of ΔH_f. Chan *et al*. reported the ΔE_f of CEL-NIC to be +0.36 kcal/mol, or +3.0 J/g, from lattice energy calculation.[15] The optimized co-crystal structure used in the calculation was the same as our single crystal structure. Therefore, both analyses agreed that the formation process of CEL-NIC is endothermic, different from other NIC co-crystals (34 co-crystals with calculated ΔE_f data and 4 co-crystals with experimental ΔH_f data[15,26]). It is noteworthy that most experimentally analyzed co-crystals have negative ΔH_f and ΔG_f, as we will discuss later.

Determination of ΔG_f from solubility measurements. An endothermic ΔH_f would raise a question of whether the co-crystal formation is thermodynamically preferred ($\Delta G_f < 0$). We measured the solubility of CEL, NIC, a physical mixture of 1:1 ratio, and the co-crystal in chloroform at 25 °C (Table 3). We found the solubility of co-crystal is slightly lower than the physical mixture, indicating that the co-crystal is more stable. On the other hand, the solubility of the physical mixture is significantly higher than individual components, showing the solubility enhancement effect which had previously

Table 3. Solubility of CEL, NIC, 1:1 physical mixture, and co-crystal in chloroform at 25 °C

Phase	CEL, mg/ml	NIC, mg/ml
CEL	32.2 (0.5)	-
NIC	-	6.6 (0.1)
1:1 physical mixture[a]	64.4 (0.9)	14.2 (0.3)
Co-crystal[b]	55.5 (0.8)	13.6 (0.2)

[a]Concentration of CEL and NIC after 1 day of dissolution when co-crystal was not yet formed in the excess solids (Figure S1a)
[b]Excess solids contained co-crystal and NIC (Figure S1b)

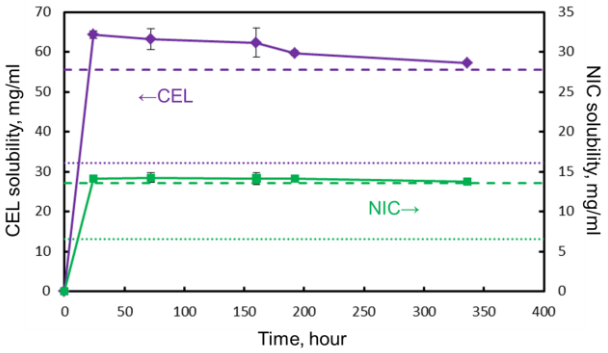

Figure 3. Dissolution profiles of a 1:1 physical mixture of CEL and NIC in chloroform at 25 °C. Equilibrium solubility of pure CEL (32.2 mg/ml) or pure NIC (6.6 mg/ml) is indicated by dotted lines. Equilibrium solubility of CEL-NIC co-crystal (CEL, 55.5 mg/ml; NIC, 13.6 mg/ml) is indicated by dashed lines. CEL-NIC co-crystal was found in the solid phase after 192 hour (8 day) of dissolution.

been reported for NIC.[37] No phase change was observed through the experiment except for the co-crystal, where excess NIC was formed along with the remaining co-crystal as a result of incongruent dissolution (Figure S1b). ΔG_f of the co-crystal was determined to be -0.7 (0.1) J/g at 25 °C (equation 5).

The negative ΔG_f suggests that at 25 °C, formation of the co-crystal is thermodynamically favored. This was further examined by continuing agitation of the physical mixture in chloroform at the same temperature. As shown in Figure 3, a slight decrease in concentration towards the equilibrium solubility of the co-crystal was observed after the initial plateau. Phase change in excess solids was also found during the experiment (Figure S1a). Co-crystal started to form in the excess solids between 160-192 hours of agitation, while excess CEL disappeared at t = 336 hours showing the co-crystallization was complete. The decrease of concentration occurred simultaneously with the formation of co-crystal. Only the co-crystal and NIC were found in the excess solids at the end of the experiment. The observation of spontaneous co-crystallization supports that the co-crystal is thermodynamically stable at 25 °C.

Entropy-governed co-crystallization process. The relationship between ΔH_f, ΔS_f, and ΔG_f is reviewed in Table S1. The combination of a negative ΔG_f and a positive ΔH_f suggests that co-crystallization is entropically favored and dominated by the $-T\Delta S_f$ term. In this case, temperature plays an unusual role in co-crystal formation, as *higher* temperature would favor co-crystallization. Assuming ΔH_f and ΔS_f do not change drastically around 25 °C, a transition temperature (T_t) below 25 °C can be expected. At $T < T_t$, co-crystal will dissociate because the physical mixture is thermodynamically stable ($\Delta G_f > 0$). T_t is estimated to be around 10 °C from equation 6 based on the formation properties of CEL-NIC.

To verify this hypothesis, stability of CEL-NIC was examined in multiple conditions (Table 4). Excess amount of the co-crystal was agitated in chloroform/heptane 5/1 (v/v) in the range of 4 – 25 °C. The co-crystal was stable at 25 °C and 20 °C, but dissociated into anhydrous CEL and NIC at 15 °C and 4 °C. Therefore, the existence of a T_t between 15 – 20 °C was demonstrated. T_t is expected to be solvent independent if no solvates can be formed. Slurry competition between the co-crystal and its physical mixture was carried out in saturated solvents of Toluene and IPA/heptane 1/3 (v/v). In both solvents, co-crystal was stable at 20°C but not at 15 °C. It is therefore concluded that the relative stability between CEL-NIC and its physical mixture inverted between 15 °C and 20 °C, and the co-crystallization is controlled by entropy.

The formation of CEL-NIC is compared with other co-crystals with experimental formation properties. It should be noticed that these properties are only available for a limited number of co-crystals. As surveyed in Table 5, all co-crystals are thermodynamically favored. The CEL-NIC co-crystal, bearing a marginal favorable ΔG_f, is consistent with this trend. On the other hand, most of co-crystals are enthalpically favored except for Mefenamic acid – 4,4'-bipyridine, however the positive ΔH_f is within the experimental error.[38] Therefore, the positive ΔH_f of CEL-NIC is different from the other co-crystals.

Table 4. Stability test of CEL-NIC in multiple conditions

Starting phase	**Slurry condition**	**Ending phase**
CEL-NIC co-crystal[a]	chloroform:heptane 5:1, 25 °C, 1 day	CEL-NIC, with excess NIC
CEL-NIC co-crystal[a]	chloroform:heptane 5:1, 20 °C, 7 days	CEL-NIC, with excess NIC
CEL-NIC co-crystal[a]	chloroform:heptane 5:1, 15 °C, 7 days	CEL and NIC
CEL-NIC co-crystal[a]	chloroform:heptane 5:1, 4 °C, 5 days	CEL and NIC
CEL-NIC co-crystal, CEL, NIC[b]	toluene, 20 °C, 1 day	CEL-NIC
CEL-NIC co-crystal, CEL, NIC[b]	toluene, 15 °C, 1 day	CEL and NIC
CEL-NIC co-crystal, CEL, NIC[b]	IPA:heptane 1:3, 20 °C, 1 day	CEL-NIC
CEL-NIC co-crystal, CEL, NIC[b]	IPA:heptane 1:3, 15 °C, 1 day	CEL and NIC

[a]For experiments in chloroform:heptane, slurry was formed by adding excess amount of CEL-NIC into the solvent.
[b]For experiments in toluene or IPA:heptane, saturated solvents with CEL and NIC were used.

Table 5. Formation properties of co-crystals available in the literature

Co-crystal	Ratio	T, °C	ΔG_f, J/g[a]	ΔH_f, J/g[a]	Reference
Celecoxib – nicotinamide	1:1	25	-0.7 (0.1)	13.0 (3.0)	This work
Carbamazepine – saccharin	1:1	33	-10.5 (0.5)[b]	-14.1 (2.1)	[11]
Bicalutamide – benzamide	1:1	25	-6.2 (0.5)	-35.5 (1.5)	[12]
Bicalutamide – salicylamide	1:1	25	-3.9 (0.5)	-20.1 (0.9)	
Carbamazepine – nicotinamide	1:1	25	-15.3 (1.8)[b]	n/a	[10]
Isonicotinamide – benzoic acid	1:1	20	-44.4 (0.7)[b]	n/a	[39]
Theophylline – oxalic acid	2:1	20	-13.5	n/a	[40]
		30	-12.5	n/a	[41]
Theophylline – glutaric acid	1:1	30	-1.2	[c]	[23]
Theophylline – salicylic acid	1:1	30	-15.5	[c]	[41]
Adefovir dipivoxil – saccharin	1:1	20	-18.9 (1.3)[b]	n/a	[42]
Proline – myricetin	2:1	25	-29.0	n/a	[43]
Nicotinamide – *R*-mandelic acid	1:1 form 1	20	n/a	-23.0 (3.0)	[13]
	1:1 form 2	20	n/a	-18.0 (3.0)	
	4:1	20	n/a	-8.0 (3.0)	[31]
	1:2	20	n/a	-20.0 (3.0)	
Nicotinamide – diflunisal	1:2	25	n/a	-40.2 (3.2)	[44]
Theophylline – diclofenac	1:1	25	n/a	-10.1 (1.9)	[45]
Theophylline – diflunisal	1:1	25	n/a	-26.0 (1.6)	
Felodipine – 4,4'-bipyridine	1:1 form 1	25	n/a	-9.6 (1.1)	[46]
	1:1 form 2	25	n/a	-5.4 (0.9)	
	2:1	25	n/a	-4.2 (0.6)	
N-phenylanthranilic acid – 4,4'-bipyridine	2:1	25	n/a	-9.6 (2.9)	[38]
Niflumic acid – 4,4'-bipyridine	2:1	25	n/a	-6.4 (0.6)	
Tolfenamic acid – 4,4'-bipyridine	2:1	25	n/a	-5.7 (0.9)	
Mefenamic acid – 4,4'-bipyridine	2:1	25	n/a	0.3 (1.3)	
Flufenamic acid – 4,4'-bipyridine	2:1	25	n/a	-11.7 (0.7)	
Melatonin – pimelic acid	1:1	50	n/a	-1.2	[47]
Vitamin D2 – vitamin D3	1:1 form 1	60	n/a	-19.1	[48]
	1:1 form 2	60	n/a	-5.9	

[a]Experimental error is only recorded when available in the reference unless otherwise noted.

[b]If ΔG_f was acquired from multiple experiments or solvent conditions, the average and standard deviation of all reported values are recorded.

[c]It was reported that ΔH_f is 98.4 J/g for theophylline – glutaric acid and 275.3 J/g for theophylline – salicylic acid.[41] The data are of doubtful reliability as they were derived from DSC thermograms with evidenced sample decomposition.

It is challenging to rationalize why the co-crystal is entropically favored from its structure. However, we propose that the entropy gain is related to the volume expansion upon co-crystallization. The formation of CEL-NIC is accompanied with one of the largest ΔV_f among all NIC co-crystals despite shorter hydrogen bonds. As the hydrophilic part of CEL molecule is reoriented to form tighter hydrogen bonds, its hydrophobic part will have to pack loosely and enjoy more freedom. In addition, the pyrazole part in the co-crystal is not hydrogen-bonded (Figure 4). We used the program Mercury (version 3.9) to analyze the occupied volume of part of CEL in CEL-NIC and in pure celecoxib (CSD#: DIBBUL[34]). In CEL-NIC, each benzyl sulfonamide group occupied 165 Å^3 of space, slightly smaller than that in pure celecoxib (175 Å^3). The reduced mobility of the hydrophilic part is in agreement with tighter hydrogen bonds. The rest of the CEL molecule, however, occupied a space of 275 Å^3 in the co-crystal, 42 Å^3 (18 %) larger than that in pure celecoxib. The increased mobility in the hydrophobic part of CEL is also evidenced by the observation of trifluoromethyl disordering in the co-crystal structure but not in pure celecoxib. It's of interest to further investigate the ΔS_f of CEL-NIC and other co-crystals with a large volume expansion upon formation.

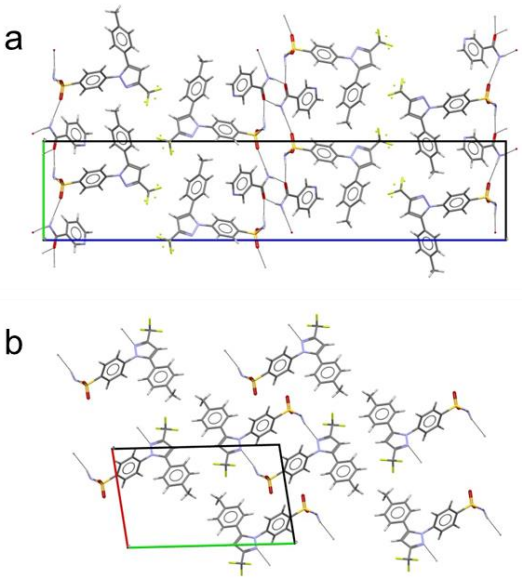

Figure 4. Packing diagrams of (a) CEL-NIC co-crystal (22 °C structure) and (b) CEL crystal (CSD#: DIBBUL, solved at room temperature). Disordered trifluoromethyl group is observed only in the co-crystal structure.

The fact that co-crystallization can be controlled by entropy may affect the current practices in co-crystal screening and synthesis. First of all, lattice energy calculation has been widely used

in virtual co-crystal screening and structure prediction, with the hypothesis that formation energy (ΔE_f, $\approx \Delta H_f$) dominates the co-crystal formation.[15,17] However, this work indicates that pairs of components with unfavorable ΔE_f should not be automatically eliminated from further consideration, especially when the energy difference is marginal. Wet-lab screening should be applied to those cases for verification. On the other hand, consistent efforts are needed for the development of ΔG_f-based computational methods to better evaluate co-crystal formation, as ΔE_f term is found to be inconclusive and insufficient in the study of CEL-NIC.[15]

Secondly, thermodynamic properties are vital in the selection of crystallization condition as the crystallization outcome is affected. Direct crystallization from super-saturated solution and slurry conversion are widely used in the isolation of organic solids. To induce super-saturation and to increase the yield, temperature reduction and anti-solvent addition are preferred over solvent evaporation at the industrial scale. However, the existence of a T_t below the co-crystal screening temperature – which is usually room temperature – will bring uncertainty to the cooling crystallization outcomes. This is similar to the existence of enantiotropically related polymorphs narrows down the operational temperature range for acquiring a particular form. Therefore, anti-solvent addition may be a better process for entropically favored co-crystals, as the formation properties of a co-crystal are independent of solvent, as long as no solvates of components or co-crystal can be formed. It is therefore suggested that the stability or solubility of a co-crystal should be thoroughly studied at various temperatures before designing the synthetic process.[12]

This work also highlights that ΔG_f can be acquired from a single dissolution experiment with excess amount of co-crystal components (Figure 3). Dissolution will first produce a solution saturated with both components, which is also suitable for co-crystal screening.[49,50] Should the

co-crystal be more stable than the components, the concentration of both components will decrease as co-crystal forms. The transition can be accelerated by seeding and monitored with online methods to capture the concentration change.[51] The decrease in concentration should not be confused with the "parachute-like" profile which is commonly observed for co-crystal dissolution due to recrystallization.[50] The "parachute-like" dissolution could only be observed for thermodynamically unstable phases or for a stable co-crystal in an environment that one component (usually the more soluble one – the co-former) is undersaturated.[12] A stable co-crystal will not dissociate into a physical mixture in non-solvating solvents or in the solid state.

CONCLUSION

This study revisited the co-crystal containing celecoxib and nicotinamide and identified its remarkable formation process which is driven by entropy. A single crystal structure is reported, which agrees with the structural optimization of Chan *et al.*[15] and allows the comparison between experimental and computational investigations. The ΔH_f of the co-crystal was determined from its melting enthalpy and that of the physical mixture of component crystals. The ΔG_f of the co-crystal was determined from solubility data. We find that the formation of CEL-NIC co-crystal increases enthalpy, in agreement with computational simulation but distinct from other NIC co-crystals and co-crystals with reported formation enthalpies. This peculiarity is further supported by the fact that co-crystal formation is thermodynamically favorable at 25 °C, resulting in the conclusion that the co-crystallization is entropically driven. The existence of a transition temperature (T_t) below 25 °C which inverts the stability between the co-crystal and physical mixture was predicted by the thermodynamic formation properties and confirmed experimentally, further supporting this conclusion.

The entropy-driven formation process of CEL-NIC not only enriches our understanding on the mechanism of co-crystallization but also brings new opportunities into co-crystal research and development. It challenges the usage of ΔE_f or ΔH_f as a primary indicator of co-crystal formation during computational simulation, and encourages new methods or algorithms with incorporation of the entropy effect. It questions the usage of temperature reduction during process development as a way to form co-crystals, as the co-crystal phase may not be favored at lower temperature. It is suggested that the thermodynamic properties of a co-crystal should be thoroughly studied at process temperatures to avoid unexpected outcomes. This study emphasizes the importance of thermodynamic studies as a valuable complement to structural and kinetic investigations in understanding the formation and stability of co-crystals.

ASSOCIATED CONTENT

Supporting Information

XRPD patterns of excess solids during the dissolution of physical mixture or co-crystal; the correlation between ΔG_f, ΔH_f, and ΔS_f; calculation method of the change of hydrogen-bond length upon co-crystallization (ΔR_{HB}) for CEL-NIC co-crystal; crystallographic data and structure refinement for CEL-NIC co-crystal (100K and 293K)

Accession Codes

CCDC 1532378 and 1532379 contain the supplementary crystallographic data for this paper. These data can be obtained free of charge via www.ccdc.cam.ac.uk/data_request/cif, or by emailing data_request@ccdc.cam.ac.uk, or by contacting The Cambridge Crystallographic Data Centre, 12, Union Road, Cambridge CB2 1EZ, UK; fax: +44 1223 336033.

AUTHOR INFORMATION

Corresponding Author

*E-mail: siwei.zhang@merck.com. Phone: +1 (732) 594 9127.

ORCID

Siwei Zhang: 0000-0001-8677-3722

Notes

The authors declare no competing financial interest.

ACKNOWLEDGEMENTS

S.-W. Z. thanks C. Scott Shultz for providing the optimized synthetic route of CEL-NIC co-crystal. S-W. Z. thanks Alfred Lee and Narayan Variankaval for helpful discussions.

REFERENCES

1. Aakeroy, C. B.; Forbes, S.; Desper, J. *J. Am. Chem. Soc.* **2009,** *131*, 17048-17049.

2. Karki, S.; Friscic, T.; Fabian, L.; Laity, P. R.; Day, G. M.; Jones, W. *Adv. Mater.* **2009,** *21*, 3905-3909.

3. Ferretti, V.; Dalpiaz, A.; Bertolasi, V.; Ferraro, L.; Beggiato, S.; Spizzo, F.; Spisni, E.; Pavan, B. *Mol. Pharmaceut.* **2015,** *12*, 1501-1511.

4. Li, Z.; Matzger, A. J. *Mol. Pharmaceut.* **2016,** *13*, 990-995.

5. Bolton, O.; Matzger, A. J. *Angew. Chem. Int. Edit.* **2011,** *50*, 8960-8963.

6. Childs, S. L.; Chyall, L. J.; Dunlap, J. T.; Smolenskaya, V. N.; Stahly, B. C.; Stahly, G. P. *J. Am. Chem. Soc.* **2004,** *126*, 13335-13342.

7. McNamara, D. P.; Childs, S. L.; Giordano, J.; Iarriccio, A.; Cassidy, J.; Shet, M. S.; Mannion, R.; O'Donnell, E.; Park, A. *Pharm. Res.* **2006,** *23*, 1888-1897.

8. Cherukuvada, S.; Kaur, R.; Row, T. N. G. *CrystEngComm* **2016,** *18*, 8528-8555.

9. Li, Z. B.; Yang, B. S.; Jiang, M.; Eriksson, M.; Spinelli, E.; Yee, N.; Senanayake, C. *Org. Process Res. Dev.* **2009,** *13*, 1307-1314.

10. Schartman, R. R. *Int. J. Pharmaceut.* **2009,** *365*, 77-80.

11. Oliveira, M. A.; Peterson, M. L.; Davey, R. J. *Cryst. Growth Des.* **2011,** *11*, 449-457.

12. Surov, A. O.; Solanko, K. A.; Bond, A. D.; Bauer-Brandl, A.; Perlovich, G. L. *CrystEngComm* **2016,** *18*, 4818-4829.

13. Zhang, S.-W.; Guzei, I. A.; de Villiers, M. M.; Yu, L.; Krzyzaniak, J. F. *Cryst. Growth Des.* **2012,** *12*, 4090-4097.

14. Perlovich, G. L. *CrystEngComm* **2015,** *17*, 7019-7028.

15. Chan, H. C. S.; Kendrick, J.; Neumann, M. A.; Leusen, F. J. J. *CrystEngComm* **2013,** *15*, 3799-3807.

16. Chan, H. C. S.; Woollam, G. R.; Wagner, T.; Schmidt, M. U.; Lewis, R. A. *CrystEngComm* **2014,** *16*, 4365-4368.

17. Abramov, Y. A.; Loschen, C.; Klamt, A. *J. Pharm. Sci.* **2012,** *101*, 3687-3697.

18. Berry, D. J.; Seaton, C. C.; Clegg, W.; Harrington, R. W.; Coles, S. J.; Horton, P. N.; Hursthouse, M. B.; Storey, R.; Jones, W.; Friscic, T.; Blagden, N. *Cryst. Growth Des.* **2008,** *8*, 1697-1712.

19. Cherukuvada, S.; Row, T. N. G. *Cryst. Growth Des.* **2014,** *14*, 4187-4198.

20. Xu, J.; Huang, Y.; Ruan, S.; Chi, Z.; Qin, K.; Cai, B.; Cai, T. *CrystEngComm* **2016,** *18*, 8776-8786.

21. Jayasankar, A.; Reddy, L. S.; Bethune, S. J.; Rodriguez-Hornedo, N. *Cryst. Growth Des.* **2009,** *9*, 889-897.

22. Guo, K.; Sadiq, G.; Seaton, C.; Davey, R.; Yin, Q. X. *Cryst. Growth Des.* **2010,** *10*, 268-273.

23. Zhang, S.; Rasmuson, A. C. *Cryst. Growth Des.* **2013,** *13*, 1153-1161.

24. Price, S. L. *Chem. Soc. Rev.* **2014,** *43*, 2098-2111.

25. Braun, D. E.; Ardid-Candel, M.; D'Oria, E.; Karamertzanis, P. G.; Arlin, J.-B.; Florence, A. J.; Jones, A. G.; Price, S. L. *Cryst. Growth Des.* **2011,** *11*, 5659-5669.

26. Zhang, S. W.; Kendrick, J.; Leusen, F. J. J.; Yu, L. *J. Pharm. Sci.* **2014,** *103*, 2896-2903.

27. Seaton, C. C.; Parkin, A. *Cryst. Growth Des.* **2011,** *11*, 1502-1511.

28. Remenar, J. F.; Peterson, M. L.; Stephens, P. W.; Zhang, Z.; Zimenkov, Y.; Hickey, M. B. *Mol. Pharmaceut.* **2007,** *4*, 386-400.

29. Lu, G. W.; Hawley, M.; Smith, M.; Geiger, B. M.; Pfund, W. *J. Pharm. Sci.* **2006,** *95*, 305-317.

30. Li, J. J.; Bourne, S. A.; Caira, M. R. *Chem. Commun.* **2011,** *47*, 1530-1532.

31. Zhang, S.-W.; Harasimowicz, M. T.; de Villiers, M. M.; Yu, L. *J. Am. Chem. Soc.* **2013,** *135*, 18981-18989.

32. Etter, M. C.; Macdonald, J. C.; Bernstein, J. *Acta Crystallogr. B-Struct. Sci.* **1990,** *46*, 256-262.

33. Bernstein, J.; Davis, R. E.; Shimoni, L.; Chang, N. L. *Angew. Chem. Int. Edit.* **1995,** *34*, 1555-1573.

34. Vasu Dev, R.; Shashi Rekha, K.; Vyas, K.; Mohanti, S. B.; Rajender Kumar, P.; Om Reddy, G. *Acta Crystallogr. C* **1999,** *55*, IUC9900161.

35. Miwa, Y.; Mizuno, T.; Tsuchida, K.; Taga, T.; Iwata, Y. *Acta Crystallogr. B* **1999,** *55*, 78-84.

36. Chawla, G.; Gupta, P.; Thilagavathi, R.; Chakraborti, A. K.; Bansal, A. K. *Eur. J. Pharm. Sci.* **2003,** *20*, 305-317.

37. Handa, Y. P.; Benson, G. C. *Fluid Phase Equilibr.* **1979,** *3*, 185-249.

38. Surov, A. O.; Simagina, A. A.; Manin, N. G.; Kuzmina, L. G.; Churakov, A. V.; Perlovich, G. L. *Cryst. Growth Des.* **2015,** *15*, 228-238.

39. Boyd, S.; Back, K.; Chadwick, K.; Davey, R. J.; Seaton, C. C. *J. Pharm. Sci.* **2010,** *99*, 3779-3786.

40. Zhang, S.; Rasmuson, A. C. *CrystEngComm* **2012,** *14*, 4644-4655.

41. Zhang, S.; Chen, H.; Rasmuson, A. C. *CrystEngComm* **2015,** *17*, 4125-4135.

42. Ma, K.; Zhang, Y.; Kan, H. L.; Cheng, L. F.; Luo, L.; Su, Q.; Gao, J.; Gao, Y.; Zhang, J. J. *Pharm. Res.* **2014,** *31*, 1766-1778.

43. Liu, M. Y.; Hong, C.; Yao, Y. S.; Shen, H. Y.; Ji, G.; Li, G. W.; Xie, Y. *Eur. J. Pharm. Biopharm.* **2016,** *107*, 151-159.

44. Evora, A. O. L.; Castro, R. A. E.; Maria, T. M. R.; Silva, M. R.; ter Horst, J. H.; Canotilho, J.; Eusebio, M. E. S. *Int. J. Pharmaceut.* **2014,** *466*, 68-75.

45. Surov, A. O.; Voronin, A. P.; Manin, A. N.; Manin, N. G.; Kuzmina, L. G.; Churakov, A. V.; Perlovich, G. L. *Mol. Pharmaceut.* **2014,** *11*, 3707-3715.

46. Surov, A. O.; Solanko, K. A.; Bond, A. D.; Bauer-Brandl, A.; Perlovich, G. L. *CrystEngComm* **2014,** *16*, 6603-6611.

47. Yan, Y.; Chen, J. M.; Lu, T. B. *CrystEngComm* **2015,** *17*, 612-620.

48. Wang, J. R.; Yu, Q. H.; Dai, W. J.; Mei, X. F. *Chem. Commun.* **2016,** *52*, 3572-3575.

49. Nehm, S. J.; Rodriguez-Spong, B.; Rodriguez-Hornedo, N. *Cryst. Growth Des.* **2006,** *6*, 592-600.

50. Sun, C. C. *Expert Opin. Drug Del.* **2013,** *10*, 201-213.

51. Sarraguca, M. C.; Ribeiro, P. R. S.; Dos Santos, A. O.; Lopes, J. A. *J. Pharm. Sci.* **2015,** *104*, 4099-4108.

For Table of Contents Use Only

Celecoxib-Nicotinamide Co-Crystal Revisited: Can Entropy Control Co-Crystal Formation?

Si-Wei Zhang, Andrew P. J. Brunskill, Eric Schwartz, Shuwen Sun

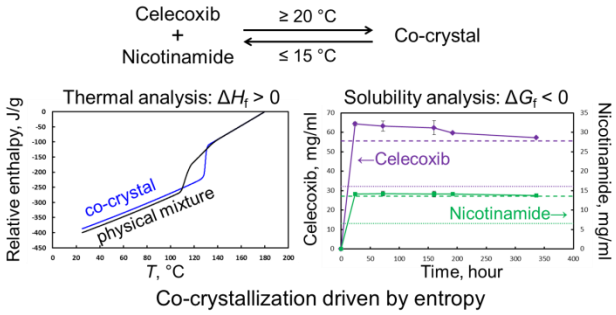

The co-crystal of celecoxib-nicotinamide has been revisited to reveal its crystal structure and unusual formation properties. Solubility and thermal analyses revealed that the formation of celecoxib-nicotinamide is endothermic and driven by entropy, a mechanism different from many reported co-crystals. The co-crystal is stable only *above* a transition temperature as predicted from thermodynamic data and confirmed experimentally.

Scheme 1. Structures of celecoxib (CEL) and nicotinamide (NIC)

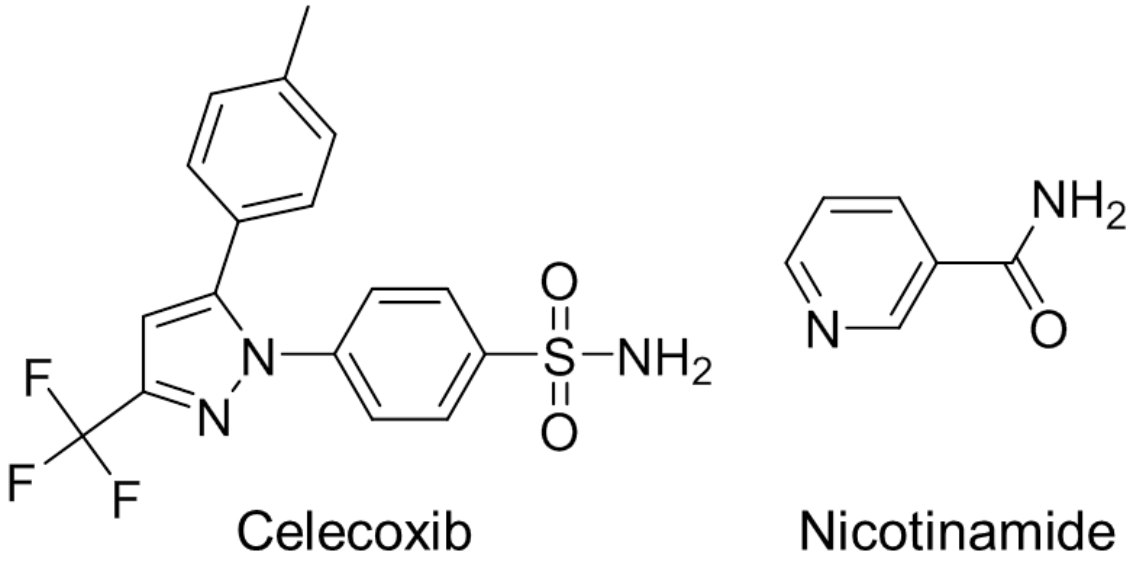

Figure 1. Hydrogen bonds in CEL-NIC co-crystal demonstrated by the 22 °C structure.

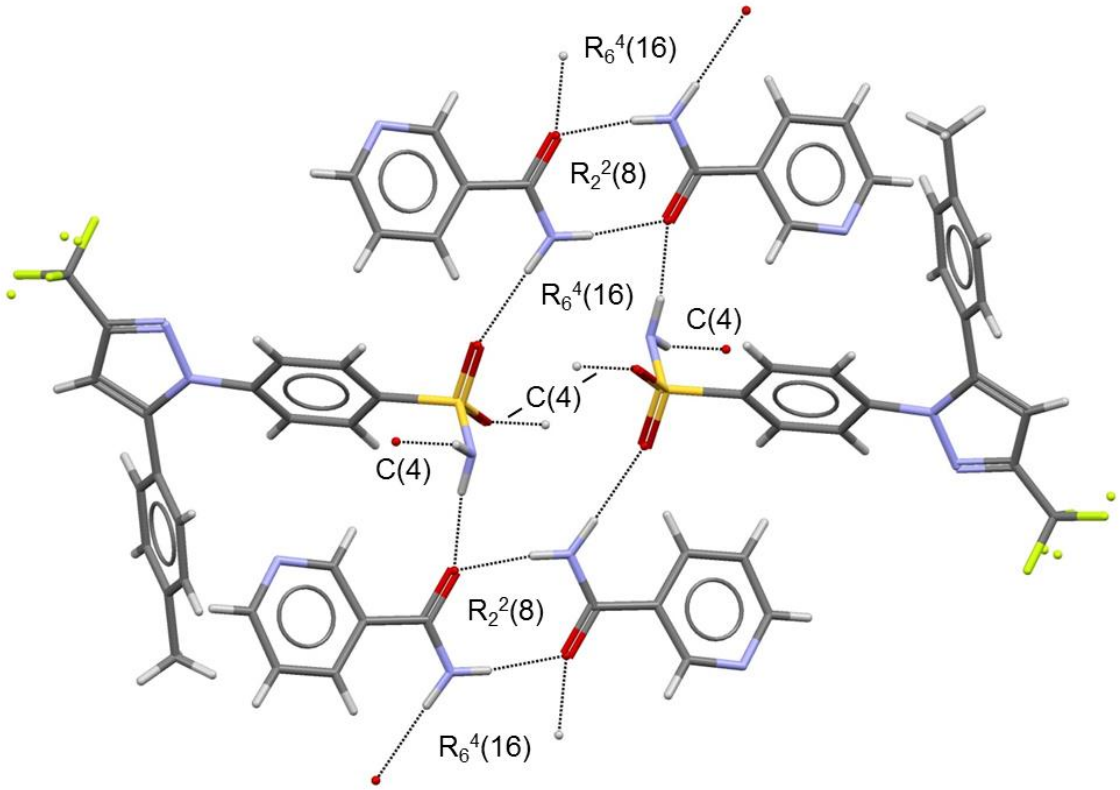

Figure 2. (a) DSC melting endotherms of CEL-NIC co-crystal, CEL, NIC, and a physical mixture of CEL and NIC at 1:1 molar ratio. (b) Relative enthalpies between co-crystal and the physical mixture. ΔH_f is the formation enthalpy of co-crystal (+13(3) J/g at 25 °C).

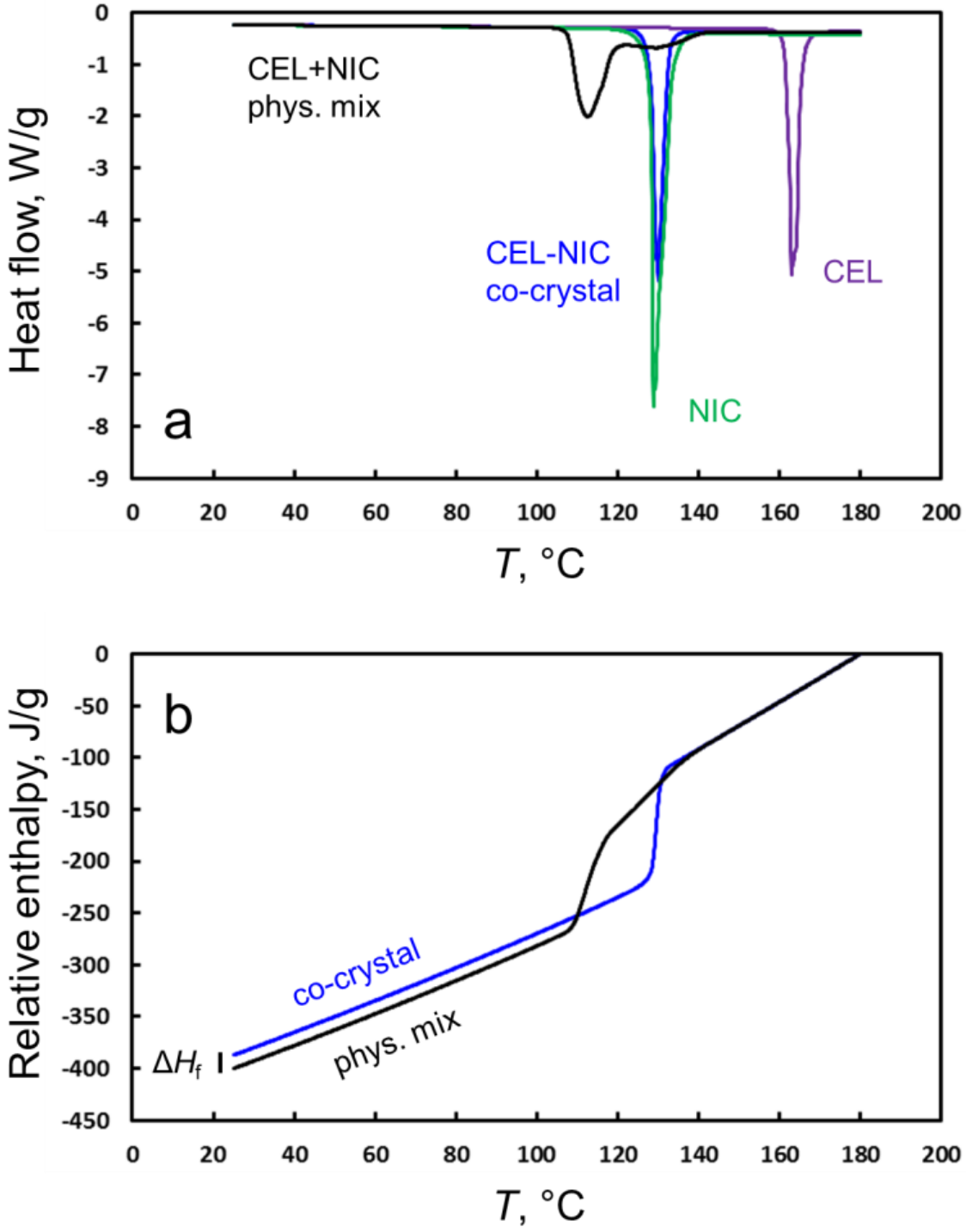

Figure 3. Dissolution profiles of a 1:1 physical mixture of CEL and NIC in chloroform at 25 °C. Equilibrium solubility of pure CEL (32.2 mg/ml) or pure NIC (6.6 mg/ml) is indicated by dotted lines. Equilibrium solubility of CEL-NIC co-crystal (CEL, 55.5 mg/ml; NIC, 13.6 mg/ml) is indicated by dashed lines. CEL-NIC co-crystal was found in the solid phase after 192 hour (8 day) of dissolution.

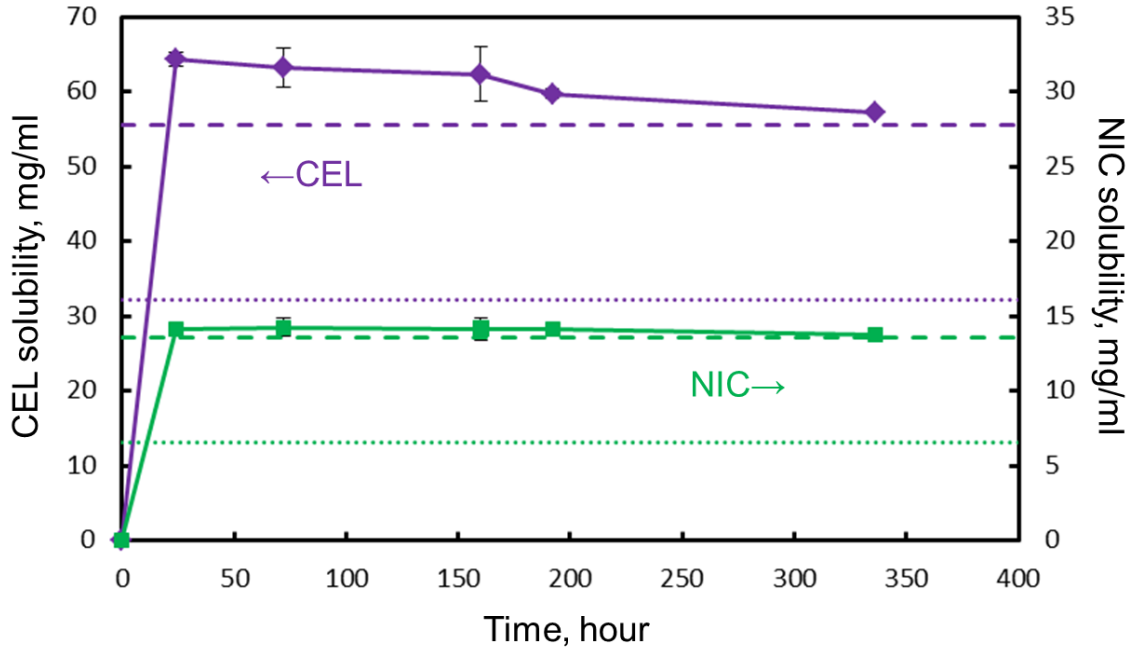

Figure 4. Packing diagrams of (a) CEL-NIC co-crystal (22 °C structure) and (b) CEL crystal (CSD#: DIBBUL, solved at room temperature). Disordered trifluoromethyl group is observed only in the co-crystal structure.

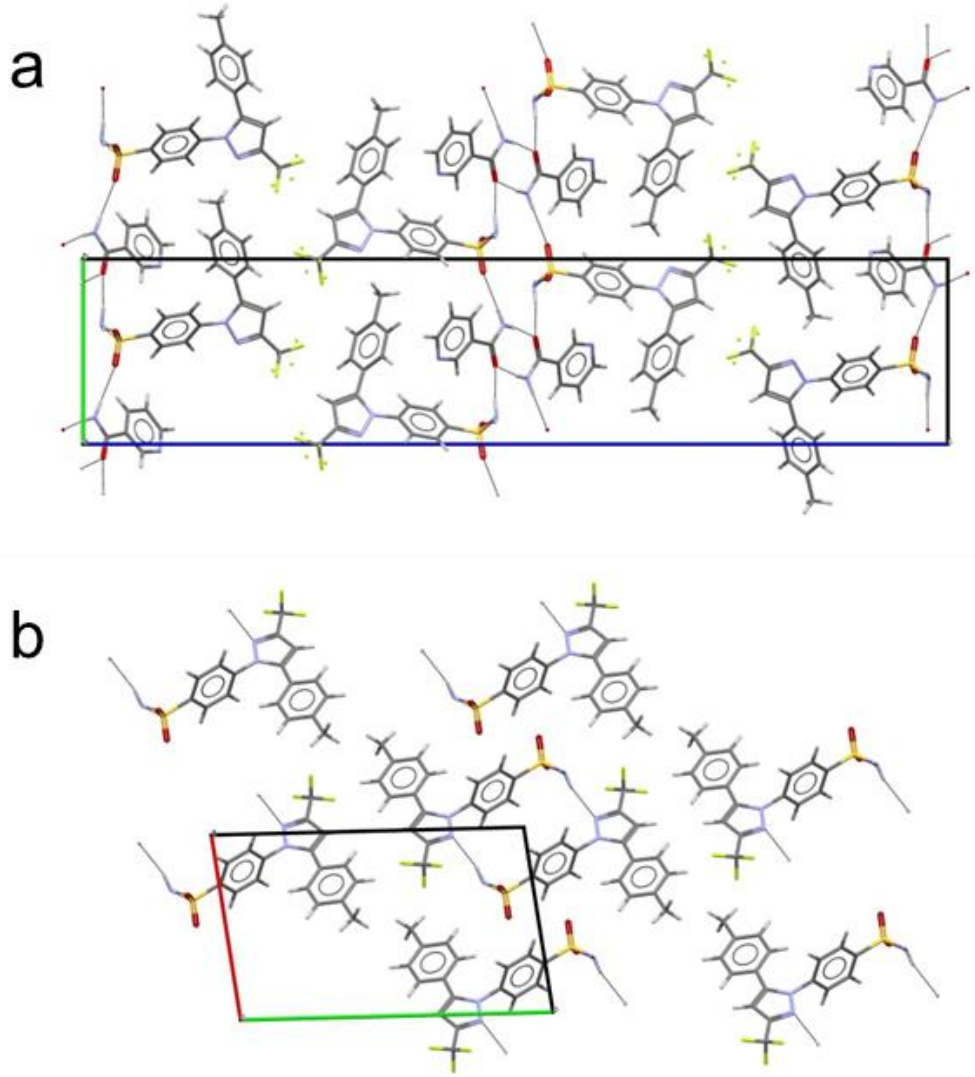

Table 1. Structures of CEL-NIC co-crystals

T, °C	-173 (2)	22 (2)
Wavelength, Å	1.54178	1.54178
Cryst system	monoclinic	monoclinic
Space group	$P\ 2_1/n$	$P\ 2_1/n$
Cryst size, mm^3	0.2×0.04×0.01	0.2×0.04×0.01
a, Å	5.1077(3)	5.1908(2)
b, Å	9.8609(5)	9.9244(4)
c, Å	46.021(2)	46.3893(16)
α, deg	90	90
β, deg	91.1948(19)	92.2545(15)
γ, deg	90	90
V, $Å^3$	2317.41	2387.92
Z	4	4
ρ, cm^3/kg	1.498	1.401

Table 2. Thermal properties of CEL, NIC, 1:1 physical mixture and co-crystal

Phase	T_m, °C	ΔH_m, J/g	T_g, °C
Celecoxib	162.3 (0.3)	101.9 (0.7)	54.4 (0.1)
Nicotinamide	128.4 (0.1)	196.3 (0.4)	–[a]
1:1 physical mixture	107.8 (0.1)	111.6 (0.5)	21.9 (0.9)
Co-crystal	128.3 (0.1)	101.1 (0.3)	21.1 (0.1)

[a] T_g could not be measured due to crystallization

Table 3. Solubility of CEL, NIC, 1:1 physical mixture, and co-crystal in chloroform at 25 °C

Phase	CEL, mg/ml	NIC, mg/ml
CEL	32.2 (0.5)	-
NIC	-	6.6 (0.1)
1:1 physical mixture[a]	64.4 (0.9)	14.2 (0.3)
Co-crystal[b]	55.5 (0.8)	13.6 (0.2)

[a]Concentration of CEL and NIC after 1 day of dissolution when co-crystal was not yet formed in the excess solids (Figure S1a)
[b]Excess solids contained co-crystal and NIC (Figure S1b)

Table 4. Stability test of CEL-NIC in multiple conditions

Starting phase	Slurry condition	Ending phase
CEL-NIC co-crystal[a]	chloroform:heptane 5:1, 25 °C, 1 day	CEL-NIC, with excess NIC
CEL-NIC co-crystal[a]	chloroform:heptane 5:1, 20 °C, 7 days	CEL-NIC, with excess NIC
CEL-NIC co-crystal[a]	chloroform:heptane 5:1, 15 °C, 7 days	CEL and NIC
CEL-NIC co-crystal[a]	chloroform:heptane 5:1, 4 °C, 5 days	CEL and NIC
CEL-NIC co-crystal, CEL, NIC[b]	toluene, 20 °C, 1 day	CEL-NIC
CEL-NIC co-crystal, CEL, NIC[b]	toluene, 15 °C, 1 day	CEL and NIC
CEL-NIC co-crystal, CEL, NIC[b]	IPA:heptane 1:3, 20 °C, 1 day	CEL-NIC
CEL-NIC co-crystal, CEL, NIC[b]	IPA:heptane 1:3, 15 °C, 1 day	CEL and NIC

[a]For experiments in chloroform:heptane, slurry was formed by adding excess amount of CEL-NIC into the solvent.
[b]For experiments in toluene or IPA:heptane, saturated solvents with CEL and NIC were used.

Table 5. Formation properties of co-crystals available in the literature

Co-crystal	Ratio	T, °C	ΔG_f, J/g[a]	ΔH_f, J/g[a]	Reference
Celecoxib – nicotinamide	1:1	25	-0.7	13.0 (3.0)	This work
Carbamazepine – saccharin	1:1	33	-10.5 (0.5)[b]	-14.1 (2.1)	[11]
Bicalutamide – benzamide	1:1	25	-6.2 (0.5)	-35.5 (1.5)	[12]
Bicalutamide – salicylamide	1:1	25	-3.9 (0.5)	-20.1 (0.9)	
Carbamazepine – nicotinamide	1:1	25	-15.3 (1.8)[b]	n/a	[10]
Isonicotinamide – benzoic acid	1:1	20	-44.4 (0.7)[b]	n/a	[39]
Theophylline – oxalic acid	2:1	20	-13.5	n/a	[40]
		30	-12.5	n/a	[41]
Theophylline – glutaric acid	1:1	30	-1.2	[c]	[23]
Theophylline – salicylic acid	1:1	30	-15.5	[c]	[41]
Adefovir dipivoxil – saccharin	1:1	20	-18.9 (1.3)[b]	n/a	[42]
Proline – myricetin	2:1	25	-29.0	n/a	[43]
Nicotinamide – *R*-mandelic acid	1:1 form 1	20	n/a	-23.0 (3.0)	[13]
	1:1 form 2	20	n/a	-18.0 (3.0)	
	4:1	20	n/a	-8.0 (3.0)	[31]
	1:2	20	n/a	-20.0 (3.0)	
Nicotinamide – diflunisal	1:2	25	n/a	-40.2 (3.2)	[44]
Theophylline – diclofenac	1:1	25	n/a	-10.1 (1.9)	[45]
Theophylline – diflunisal	1:1	25	n/a	-26.0 (1.6)	
Felodipine – 4,4'-bipyridine	1:1 form 1	25	n/a	-9.6 (1.1)	[46]
	1:1 form 2	25	n/a	-5.4 (0.9)	
	2:1	25	n/a	-4.2 (0.6)	
N-phenylanthranilic acid – 4,4'-bipyridine	2:1	25	n/a	-9.6 (2.9)	[38]
Niflumic acid – 4,4'-bipyridine	2:1	25	n/a	-6.4 (0.6)	
Tolfenamic acid – 4,4'-bipyridine	2:1	25	n/a	-5.7 (0.9)	
Mefenamic acid – 4,4'-bipyridine	2:1	25	n/a	0.3 (1.3)	
Flufenamic acid – 4,4'-bipyridine	2:1	25	n/a	-11.7 (0.7)	
Melatonin – pimelic acid	1:1	50	n/a	-1.2	[47]
Vitamin D2 – vitamin D3	1:1 form 1	60	n/a	-19.1	[48]
	1:1 form 2	60	n/a	-5.9	

[a]Experimental error is only recorded when available in the reference unless otherwise noted.

[b]If ΔG_f was acquired from multiple experiments or solvent conditions, the average and standard deviation of all reported values are recorded.

[c]It was reported that ΔH_f is 98.4 J/g for theophylline – glutaric acid and 275.3 J/g for theophylline – salicylic acid.[41] The data are of doubtful reliability as they were derived from DSC thermograms with evidenced sample decomposition.

TOC Graphic

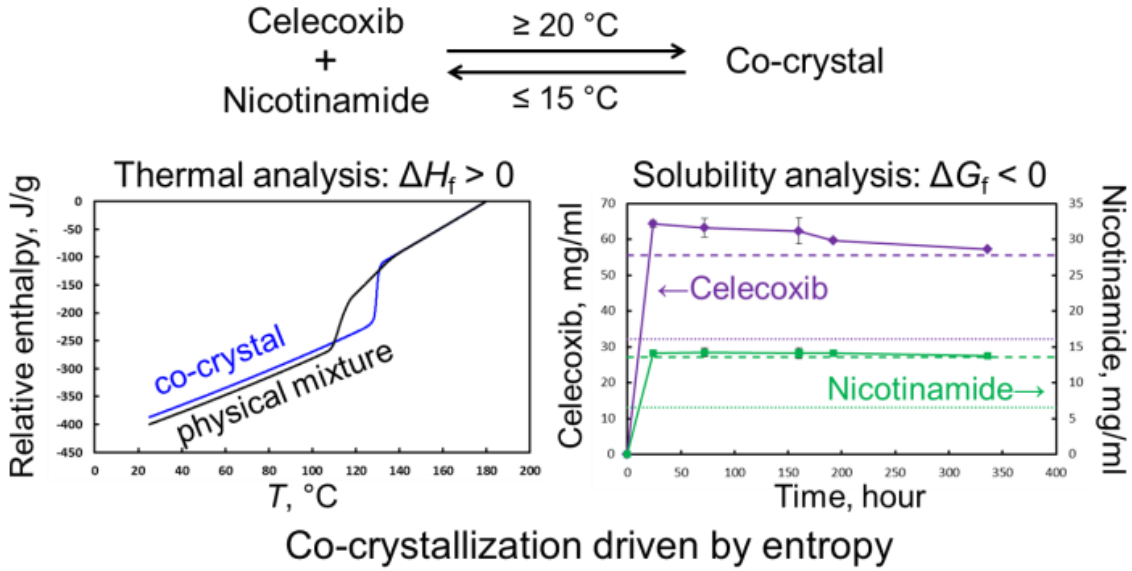
Celecoxib
+
Nicotinamide
≥ 20 °C
≤ 15 °C
Co-crystal
Thermal analysis: ΔH_f > 0
Relative enthalpy, J/g
co-crystal
physical mixture
T, °C
Solubility analysis: ΔG_f < 0
Celecoxib, mg/ml
Nicotinamide, mg/ml
←Celecoxib
Nicotinamide→
Time, hour
Co-crystallization driven by entropy